Efficacy of neuraminidase inhibitors against H5N6 highly pathogenic avian influenza virus in a non-human primate model

Running title: NA inhibitors against H5N6 influenza virus in macaques

Cong Thanh Nguyen[1], Saori Suzuki[1], Yasushi Itoh[1,*], Hirohito Ishigaki[1], Misako Nakayama[1], Kaori Hayashi[1, 2], Keita Matsuno[3,4], Masatoshi Okamatsu[3], Yoshihiro Sakoda[3,4], Hiroshi Kida[5] & Kazumasa Ogasawara[1,6]

[1] Division of Pathogenesis and Disease Regulation, Department of Pathology, Shiga University of Medical Science, Otsu 520-2192, Japan

[2] Department of Gynecology, Shiga University of Medical Science, Otsu 520-2192, Japan

[3] Laboratory of Microbiology, Department of Disease Control, Faculty of Veterinary Medicine, Hokkaido University, Sapporo 060-0818, Japan

[4] Global Station for Zoonosis Control, Global Institution for Collaborative Research and Education (GI-CoRE), Hokkaido University, Sapporo 060-0818, Japan

[5] Research Center for Zoonosis Control, Hokkaido University, Sapporo 001-0020, Japan

[6] Research Center for Animal Life Science, Shiga University of Medical Science, Otsu 520-2192, Japan

[*] Corresponding author

E-mail: yasushii@belle.shiga-med.ac.jp (YI)

Abstract

Attention has been paid to H5N6 highly pathogenic avian influenza virus (HPAIV) because of its heavy burden on the poultry industry and human mortality. Since an influenza A virus carrying N6 neuraminidase (NA) has never spread in humans, the potential for H5N6 HPAIV to cause disease in humans and the efficacy of antiviral drugs against the virus need to be urgently assessed. We used non-human primates to elucidate the pathogenesis of H5N6 HPAIV as well as to determine the efficacy of antiviral drugs against the virus. H5N6 HPAIV infection led to high fever in cynomolgus macaques. The lung injury caused by the virus was severe with diffuse alveolar damage and neutrophil infiltration. In addition, an increase in IFN-α showed an inverse correlation with virus titers during the infection process. Oseltamivir was effective for reducing H5N6 HPAIV propagation, and continuous treatment with peramivir reduced virus propagation and severity of symptoms in the early stage. This study also showed the pathologically severe lung injury states in the cynomolgus macaques infected with H5N6 HPAIV, even in those that received early antiviral drug treatments, indicating the need for close monitoring and the need for further studies on the virus pathogenicity and new antiviral therapies.

Introduction

Global epidemics of highly pathogenic avian influenza viruses (HPAIVs) have been continuing. The number of subtypes detected in domestic birds and the number of countries affected by HPAIVs are larger than those in past epidemics (2005-2012) (1). By genetic reassortment, new gene combinations of influenza viruses may create a high risk to human health due to an increase of the transmission ability and antiviral drug resistance (2-4). The novel HPAIV of subtype H5N6 that has been detected since 2013 is associated with human mortality

and has caused a great burden on the poultry industry (5-7). Nineteen humans were infected with H5N6 HPAIV and 13 of them died (fatality rate of 68.4%) (7). The hemagglutinin (HA) protein of reported H5N6 HPAIVs have both affinity for human-like (α2,6) and avian-like (α2,3) sialic acid receptors, suggesting that H5N6 HPAIV has high potential for avian-human transmission (8-10). In addition, this subtype virus was transmitted among mammalians by a direct contact route and was found in wild birds, especially migratory waterfowl that transverse long distances, posing a potential threat for wide dissemination of this virus (1, 10).

The pathogenesis of H5N6 HPAIV is controversial and remains to be elucidated. One study in mice and ferrets showed that H5N6 HPAIV was less pathogenic than the other H5 HPAIVs (8). On the other hand, it was shown that H5N6 HPAIV caused more severe disease in ferrets than did other H5 clade 2.3.4.4 viruses (11). Another study in ferrets also showed the different pathogenicities among H5N6 HPAIVs (10). The pathogenic characteristics of H5N6 HPAIV must be determined more clearly, especially in models for which the pathogenicity can be extrapolated to humans.

The state of antiviral drug resistance increases with evolution of an influenza virus. Neuraminidase inhibitors (NAIs) are currently recommended for treatment of most the influenza A viruses, but some NAI resistance-conferring mutations have been reported (12-14). The majority of seasonal influenza A viruses are resistant to M2 ion channel inhibitors, but the frequency and distribution of amantadine (AMT)-resistant influenza variants depends on HA subtypes, host species, years of isolation and geographical areas (12, 14, 15). The efficacy of antiviral drugs against H5N6 HPAIV, the first influenza A virus carrying N6 NA found in humans, is unknown. Therefore, the efficacy of available and easily accessible antiviral drugs such as NAIs and M2 ion channel inhibitors should be clarified in *in vivo* studies.

In the present study, we used the cynomolgus macaque model to investigate the pathogenicity and antiviral susceptibility of H5N6 HPAIV A/black swan/Akita/1/2016 (H5N6). Cynomolgus macaques were used because of their high genetic similarity to humans as well as their symptoms and histopathologic findings that are similar to those in humans infected with influenza viruses (16-18). The present study showed that H5N6 HPAIV caused severe pneumonia in macaques, even in those that received early treatments with NAIs. Oseltamivir (OTV) was effective for reducing H5N6 HPAIV propagation, and continuous treatment with peramivir (PRV) reduced the virus propagation and symptoms effectively in the early stage. However, AMT had no effect on early reduction of virus titers.

Results

Virus replication in the respiratory tracts of cynomolgus macaques infected with H5N6 HPAIV. Firstly, we investigated the replication of A/black swan/Akita/1/2016 (H5N6) virus in the macaques' respiratory tracts (19, 20). Virus was detected in the control group intragastrically and intravenously treated with saline until day 7 in swab samples from the nasal cavity and trachea and until day 6 in bronchial samples (Table 1 and Table S1). In the nasal cavity, the virus titer increased with a peak on day 6. In the groups treated with intragastric oseltamivir phosphate (30 mg/kg) or intravenous peramivir hydrate (30 mg/kg) for 5 days, no virus was detected on day 7 in the swab samples. The virus titers in NAI treatment groups were lower than that in the control group after day 5. Meanwhile, in the group treated with intragastric AMT (10 mg/kg) continuously for 5 days, the virus titers were comparable to those in the control group, although the M2 gene of the inoculum virus (GenBank LC198539.1) indicated sensitivity to AMT (19). Viruses were found in macaque A2 (nasal cavity) and macaque A3 (trachea, bronchus) on day 7

(Table 1). The virus titer areas under the concentration-time curves (AUC, the summation of virus titers from day 1 to day 7 and from day 2 to day 7), in the nasal swabs of the groups treated with PRV and OTV was significantly lower than that in the control group (Fig. S1). The AUC in the AMT-treated group was comparable to that in the control group. Thus, H5N6 HPAIV propagated in the macaques, and NAIs, not AMT, were effective for early reduction of virus titers.

Tissues of the respiratory tract were used to determine the presence of H5N6 HPAIV on day 7 after virus infection (Table S2). We detected the virus in both upper respiratory tissues and lower respiratory tissues in the control group. A very small amount of virus was detected in the group treated with OTV. The AMT-treated group had much less virus titers than those in the control group in the upper respiratory tracts on day 7. Meanwhile, more virus was detected in tonsils and lower respiratory samples in the PRV-treated group, and we did not find any NAI-resistant mutation that has been reported such as E119V, I222L, R292K, and R371K (data not shown) (13, 21). No mutation associated with AMT resistance was detected in the genes of the virus recovered on day 7 in samples from the macaques treated with AMT (both tissues and swab samples) (data not shown). No virus was detected in other organs including the mediastinum lymph nodes, heart, spleen, kidney, liver, conjunctiva, and brain (data not shown).

Clinical signs in cynomolgus macaques infected with H5N6 HPAIV. To examine the clinical signs caused by infection of H5N6 HPAIV, body temperatures in the macaques were monitored. After H5N6 HPAIV infection, body temperatures in the macaques were very high (Fig. 1a). Body temperatures in 12 macaques increased by 3.0 ^{o}C on average on the first night after virus inoculation. After that, body temperatures decreased by about 1.5 ^{o}C on day 2 and then remained

115 unchanged until day 5 and decreased on day 7. The body temperatures in the group treated with
116 PRV were lower than those in the control group on day 1, day 3, and day 4 after virus
117 inoculation, although no significant difference was detected after treatment. OTV and AMT did
118 not reduce body temperature after H5N6 infection compared to saline. After stopping treatment,
119 the body temperatures in the groups treated with PRV and AMT increased by about 0.7 ^{o}C and
120 then decreased on day 7 (Fig. 1a).

121 Using the same telemetry system as that for measuring body temperature, we recorded
122 heart rates of the macaques throughout the experiment. Heart rate has been one of the criteria for
123 estimating the efficacy of antiviral treatment in clinical trials (22). After H5N6 HPAIV infection,
124 heart rate increased from 84.4 ± 15.6 beats/min (average ± standard deviation) in night time
125 before infection to 145.7 ± 24 beats/min at night on day 0 after virus infection and did not
126 recover completely until day 6 in all groups (Fig. 1b). PRV treatment rapidly decreased the heart
127 rate, but heart rate increased on days 5 and 6. The heart rate decreased in the OTV-treated group
128 after day 3 and in the AMT-treated group only on day 6.

129 We also observed changes in appetite and the body weight in the period of infection (Fig.
130 1c, d). On the day after infection (day 1), all of the macaques left more than 50% of the food
131 pellets. Appetite started to recover after day 3 in all groups, but complete recovery on day 3 was
132 only seen in macaques treated with AMT. Appetite in the OTV group was completely recovered
133 on day 7. The food consumption had still not returned to normal on the last day in the control
134 group and the PRV group. Body weights of all macaques decreased after day 2 or 3 (Fig. 1d).
135 We did not find any significant difference in weight loss or change of appetite among the groups
136 on each day.
137

Pathological characteristics in the lungs of cynomolgus macaques 7 days after infection with H5N6 HPAIV. Viral pneumonia was histologically examined 7 days after virus inoculation. All of the macaques survived and were autopsied on day 7. Macroscopically, dark red areas indicating lung congestion were observed in the control macaques as well as in the antiviral drug-treated macaques (data not shown). Microscopically, many CD163 positive macrophages and neutrophils were present in the alveoli of the lungs of all cynomolgus macaques and the levels of lung injury appeared to be similar in the four groups (Fig. 2 and Fig. S2a). There was no significant difference of acute lung injury score among four groups (Fig. S2b). We also found a larger number of bronchus-associated lymphoid tissues (BALTs) in the group treated with AMT than in the other treated groups, although the difference was not significant. (Fig. S2c). Thus, H5N6 HPAIV caused severe pneumonia and lymphocyte responses in the lung of cynomolgus macaques.

Changes in peripheral blood cells and cytokine responses in cynomolgus macaques infected with H5N6 HPAIV. Inflammatory responses in peripheral blood after virus infection were examined. Increases in the number of total leukocytes, monocytes, and granulocytes (Fig. 3a-c) and a decrease in the number of lymphocytes (Fig. 3d) were detected on day 1 before treatment, and then they gradually returned to normal levels. In plasma, levels of IFN-α, IL-6, and MCP-1 were significantly increased on day 1 and then decreased on day 3 (Fig. 3e-g). Levels of IL-8 did not increase on day 1 but tended to increase after day 3 (Fig. 3h). Levels of IFN-γ, TNF-α, and IL-4 in plasma were increased slightly after infection (Fig. S3a-c). The increase in IL-6 had no relation to virus titers (data not shown), and we found that the increase in IFN-α was inversely correlated with virus titers in the trachea and bronchus on day 1 (Fig. 3e and Fig S4). Cytokine

responses in lung tissues were examined since severe pneumonia was observed histologically. Compared to the levels in the other three groups, high levels of IFN-γ, IL-6, MCP-1, and IL-8 were found in lung homogenates in the PRV group on day 7 (Fig. S3d-g), but there were no statistically significant differences. Thus, H5N6 HPAIV induced significant cytokine responses in peripheral blood on day 1 followed by inflammatory cytokine responses in the lung on day 7.

Efficacy of antiviral drugs against H5N6 HPAIV *in vitro*. The efficacy of the antiviral drugs was investigated in an *in vitro* study using Madin-Darby canine kidney (MDCK) cells. A/black swan/Akita/1/2016 (H5N6) was sensitive to OTV and PRV, as indicated by a decrease in virus titers when the drug concentrations were increased. At concentrations of 1 and 10 μg/mL (24 h), virus titers in the presence of PRV were significantly lower than those without PRV. Half maximal effective concentrations (EC_{50} values) at 24 h culture were 1.07 μg/mL and 0.47 μg/mL for OTV and PRV, respectively (Fig. 4a, b). AMT had no inhibitory effect on the propagation of H5N6 HPAIV even with 10 μg/mL (Fig. 4c), whereas AMT showed an inhibitory effect on the propagation of A/Aichi/2/1968 (H3N2) (Fig. S5). These results are consistent with virus titers in swab samples of treated macaques. Furthermore, the virus isolated from a tonsil of macaque P2 on day 7 was sensitive to PRV *in vitro* (Fig. 4d), as indicated by that the virus titers were significantly lower than those without treatment at PRV concentration of 1 μg/mL (both 24 h and 48 h).

Discussion

In the present study, we found that HPAIV A/black swan/Akita/1/2016 (H5N6) propagated in both the upper and lower respiratory tracts of macaques and caused severe inflammation with pneumonia and cytokine responses in the macaque model, being comparable to the severe states in humans infected with H5N6 HPAIV (7). NAIs (OTV and PRV), but not an M2 inhibitor (AMT), showed inhibitory effects on virus replication in *in vivo* and *in vitro* studies.

The macaques infected with A/black swan/Akita/1/2016 (H5N6) showed fever up to 40 ^{o}C on average and lymphopenia on day 1, similar to symptoms in H5N6 HPAIV-infected patients (7, 23). The prominent pathological characteristic of diffuse lung inflammation in the macaques was the same as that found in post-mortem studies on human cases of infection with H5N6 HPAIV and other influenza virus infections (24-27). Thus, the macaques represented human patients in clinical signs and pneumonia. However, this strain, which preferentially bound to α2,3-linked sialic acid receptors (unpublished data), propagated in both the upper and lower respiratory tracts, whereas the other H5N6 HPAIVs possessed binding affinity to both α2,6-linked sialic acid-bearing receptors and α2,3-linked receptors (8-10). Therefore, receptor-binding preference is not only a factor to determine the pathogenicity of this strain in macaques.

Cytokines/chemokines are associated with pathogenicity, relating with the disease severity of influenza infection and also potential for new therapy development (28, 29). In the present study, most of the cytokines increased in plasma of the macaques on day 1 and then decreased to normal ranges, the same as the findings on macaques infected with H5N1 HPAIV (30). IL-8 increased later (after day 3) and continued to increase until day 7. Previous studies showed that increases in IL-6 were correlated with high virus loads in the respiratory tracts and symptoms that appeared in the macaques and humans after H5N1 HPAIV infection (30, 31), but the increase in IL-6 did not show a correlation with virus titers in the present study. Differences

205 in genes and proteins other than the HA between H5N6 HPAIV used in the present study and
206 H5N1 HPAIV used in our previous study might affect cytokine responses, although further
207 studies are required to identify amino acids responsible for the differences in the future. IFN-α
208 increased significantly and was inversely correlated with virus titers, indicating that IFN-α may
209 be a protective factor against H5N6 HPAIV infection in macaques. Together with NAIs, early
210 treatment with IFN-α might be a potential therapy for H5N6 HPAIV infection as H5N1 HPAIV
211 and H7N9 virus (32, 33).

212 NAIs were effective against H5N6 HPAIV infection in the present study. The virus titers
213 in swab samples were reduced on day 5 in the groups treated with both NAIs *in vivo*. NAIs at
214 higher concentrations also inhibited virus propagation at 24 h and/or 48 h after infection *in vitro*.
215 Treatment with PRV, which resulted in rapid reduction in body temperature and heart rate,
216 seemed to be more effective than OTV in the early stage after virus infection. On day 7, the virus
217 was detected in tonsils and lung tissues of the cynomolgus macaques that had been treated with
218 PRV, and the symptoms (high body temperature, high heart rate, decreased body weight) in this
219 group did not recover well after day 5. A recent study on humans with seasonal influenza virus
220 infections showed a rebound of the virus load after stopping PRV treatment (30, 34). However,
221 no NAI-resistant mutation was found in the present and previous studies (30, 34). These results
222 suggest that additional administration of PRV is required for treatment of H5N6 HPAIV
223 infection.

224 AMT, a drug that has not been used widely for a long period of time due to rapid
225 emergence of drug resistance in seasonal influenza virus infection, did not show any effect on
226 early reduction of virus shedding compared to that in the control group in the present study,
227 although no AMT-resistant mutation was found in the M2 gene before and after virus inoculation.

Ilyushina et al reported that AMT-resistance of H7N7 HPAIVs without any M2 gene mutation was associated with the contribution of HA to the viral fusion activity (35). Therefore, the efficacy of AMT against H5N6 HPAIV might be dependent on a gene constellation and/or high pathogenicity of the virus since susceptibility of amantadine to H5 HPAIV was various among strains without amino acid residues associated with resistance of amantadine in the M2 protein (36, 37).

AMT showed no direct antiviral effects on reduction of virus titers from day 2 to day 5 during administration. However, we found lower virus titers in respiratory tissues of macaques treated with AMT than in control macaques on day 7, and this difference might be related to slight increase of BALTs in the lungs compared with other groups. AMT is a dopamine agonist that has potent effects on T cells and the disable function of regulatory T cells leads to BALT development (38, 39). Therefore, it is possible that the late efficacy of AMT for reduction of tissue virus titers is dependent on the immune response of BALT formation after viral infection instead of direct anti-viral effects of AMT.

Despite the symptomatic and virological improvements due to the antiviral treatment, the pathology finding of severe alveolar damage was not greatly different between the three treatment groups and control group. Therefore, antiviral treatment with both NAIs and an M2 inhibitor may have limited effectiveness pathologically until day 7. This study showed the need for close monitoring and the need for further studies on virus pathogenicity and the development of new antiviral therapies.

Materials and Methods

Ethnics statement. This study was done in strict accordance with the Guidelines for the Husbandry and Management of Laboratory Animals of the Research Center for Animal Life Science at Shiga University of Medical Science and Standards Relating to the Care and Fundamental Guidelines for Proper Conduct of Animal Experiments and Related Activities in Academic Research Institutions under the jurisdiction of the Ministry of Education, Culture, Sports, Science and Technology, Japan. The protocols were approved by the Shiga University of Medical Science Animal Experiment Committee (Permit Numbers: 2017-3-15(H1)). The Research Center for Animal Life Science at Shiga University of Medical Science has permission for importing cynomolgus macaques and provides regular veterinary care, monitoring, balanced nutrition and environmental enrichment. At the endpoint of 7 days after virus inoculation, the macaques were euthanized with ketamine and then intravenously injected with pentobarbital (200 mg/kg body weight). The animals were monitored every day with the clinical score system shown in Table S3 and veterinary examinations were also performed to alleviate suffering. It was decided that they would be euthanized if the scores reached 15 (a humane endpoint). Ten-day-old chicken embryonated eggs were used to propagate an inoculum virus (obtained from Sasaki Chemical, Co. Ltd., Kyoto, Japan).

Animals. Twelve healthy adult female cynomolgus macaques (*Macaca fascicularis*) (4 - 13 years old) from China, Indonesia and Vietnam were used in this study. A study schedule was shown in Table S1. To reduce suffering, ketamine (5 mg/kg) and xylazine (1 mg/kg) were used to make the animals anesthetic before collecting samples and virus inoculation. The animals were provided food pellets of CMK-2 (CLEA Japan, Inc., Tokyo, Japan) once a day after recovery from anesthesia and *ad libitum* available drinking water. The appetite percentage was

calculated in the following way: %appetite = [(number of pellets given in the morning - number of pellets left at night)/number of pellets given in the morning] × 100. Each macaque was housed individually with controlled humidity (71% - 82%), temperature (23.8 - 27.4 ^{o}C) and light (12 h light/12 h dark cycle; dark from 8:00 p.m. to 8:00 a.m.). Three weeks before virus inoculation, we implanted telemetry probes (TA10CTA-D70; Data Sciences International, St. Paul, MN) into the macaques' peritoneal cavities under anesthetic conditions with ketamine/xylazine and isoflurane inhalation in order to mainly monitor body temperature and heart rate. The macaques used in the present study were negative for herpes B virus, hepatitis E virus, *Mycobacterium tuberculosis, Shigella spp., Salmonella spp.,* and *Entamoeba histolytica*. Twelve macaques were divided into four groups: S1, S2, S3 (animal identification) macaques were treated with saline as controls; O1, O2, O3 were treated with OTV; P1, P2, P3 were treated with PRV; and A1, A2, A3 were treated with AMT. Under an anesthetic condition, swab samples were collected from the eyes, nasal cavity, oral cavity and trachea in about 30 seconds using cotton sticks from day 1 to day 7 after virus inoculation. Bronchial swab samples were collected using a bronchoscope (MEV-2560; Machida Endoscope Co. Ltd., Tokyo, Japan) and cytology brushes (BC-203D-2006; Olympus Co., Tokyo, Japan). Each of the samples (from cotton sticks and brushes) was put into 1 mL Eagle's minimal essential medium (EMEM) containing 0.1% bovine serum albumin (BSA) and antibiotics (penicillin G and streptomycin). On day 7, macaques were autopsied and tissue samples were sectioned into small pieces and stored at -80^{o}C. On the day of virus titration or tissue cytokine measurement, tissue samples were homogenized. The homogenate was adjusted with EMEM medium (0.1% BSA, penicillin, and streptomycin) into 10% weight/volume, and centrifuged at 8000 rpm for 3 min at 4 ^{o}C. The supernatants were collected and used for virus titration and cytokine measurement.

Viruses. The highly pathogenic avian influenza virus A/black swan/Akita/1/2016 (H5N6) (NCBI taxonomy ID: 1921521) was isolated from a dead black swan in a zoo (19). The virus was propagated in 10-day-old chicken embryonated eggs at 35 ^{o}C for 24 h once at Hokkaido University and once at Shiga University of Medical Science and was titrated with MDCK cells (American Type Culture Collection, Manassas, VA). The macaques were challenged with A/black swan/Akita/1/2016 (H5N6) (3×10^6 $TCID_{50}$ (50% tissue culture infective dose) in 7 mL Hanks buffer saline solution (HBSS) medium). The virus solution (0.05 mL for each conjunctiva, 0.5 mL for each nostril, 0.9 mL for the oral cavity, and 5 mL for the trachea) was inoculated on day 0. An influenza virus A/Aichi/2/1968 (H3N2) was propagated in MDCK cells. Virus titers in samples were determined as described before (40). Briefly, the MDCK cells were cultured in EMEM with 10% fetal bovine serum (FBS), penicillin G (50000 units/mL) and streptomycin (50 mg/mL) in a humidified incubator (5% CO_2 at 37 ^{o}C). MDCK cells (in cell-confluent wells) were washed twice and incubated with 100 μL sample in the multiple 10-fold dilution (quadruplicate) for 1 h in 5% CO_2 at 35 ^{o}C. Then the cells were washed with HBSS once and cultured in EMEM with 0.1% bovine serum albumin (BSA), penicillin G (50000 units/mL), and streptomycin (50 mg/mL) in a humidified incubator (5% CO_2 at 35 ^{o}C) for 3 days. Cytopathic effect (CPE) was observed with microscope. The level of detection was 0.67 $\log_{10}TCID_{50}$/mL, which means one CPE-positive well in quadruplicate culture with undiluted samples. All experiments were done under the conditions of biosafety level 3 containment of the Research Center for Animal Life Science at the Shiga University of Medical Science.

Compounds. Oseltamivir phosphate (Chugai Pharmaceutical Co., Ltd., Tokyo, Japan), peramivir hydrate (Shionogi Co., Ltd., Osaka, Japan) and amantadine hydrochloride (Symmetrel®, Tanabe Mitsubishi Co., Ltd., Osaka, Japan) were used in the *in vivo* study. Oseltamivir phosphate and amantadine phosphate were dissolved in distilled water and administrated into the stomach with a catheter (30 mg/kg and 10 mg/kg, respectively) once a day for 5 days. Peramivir phosphate (30 mg/kg) was intravenously injected into the macaques once a day for 5 days (30). Saline was administrated in cynomolgus macaques by both intragastric route and intravenous route with adjusted volumes to administration of oseltamivir (intragastric route) and peramivir (intravenous route). The doses of oseltamivir phosphate and peramivir hydrate used in the present study are doses that induce higher areas under the concentration-time curve than those standardly indicated in humans (oseltamivir phosphate at 75 mg twice a day and peramivir hydrate at 600 mg once a day) (16, 30). The dose of amantadine phosphate was higher than that recommended for pediatric patients (from 4.4 to 8.8 mg/kg/day). In *in vitro* experiments, oseltamivir carboxylate (ChemScene, LLC, Monmouth Junction, NJ), peramivir hydrate (Shionogi Co.) and amantadine hydrochloride (LKT Laboratories, Inc., MN) were used with MDCK cells. The compounds were diluted to indicated concentrations with EMEM (0.1% BSA and antibiotics) and then added to the culture of the virus-infected MDCK cells for 24 h or 48 h.

Blood cell and cytokine measurement. Peripheral blood was collected before virus infection or before antiviral drug/saline administration on days indicated in Table S1. Plasma and peripheral blood mononuclear cells and plasma were separated by Leucosep™ (Greiner bio-one) following the manufacturer's instruction and stored at -80 ^{o}C. The cell components of peripheral blood were counted by using a hemocytometer (Vetscan HMII, Abaxis, Union City, CA). Levels of

cytokines/chemokines in plasma or lung homogenate (10% weight/volume) were measured using the Milliplex MAP non-human primate cytokine panel and Luminex 200 (Millipore Corp., Billerica, MA) following the manufacturer's instructions.

Histopathological examination. Immediately after autopsy, lung tissues were fixed with 10% neutral buffered formalin. The fixed tissues were embedded in paraffin. They were then cut into 3-μm-thick sections and stained with hematoxylin and eosin (H&E). Acute lung injuries were estimated by two pathologists according to a four parameter scoring system: alveolar capillary congestion; hemorrhage; infiltration or aggregation of neutrophils in airspace or vessel wall; thickness of alveolar wall (41). Each parameter was scored from 0 to 4: 0, no or little damage; 1, lower than 25% damage; 2, 25% - 50% damage; 3, 50 - 75% damage; 4, higher than 75% damage. Totally 8 H&E staining sections for each macaque's lung were examined (one section from upper and middle lobes and two sections from lower lobes in bilateral lungs). Averages of three macaques was used to compare the acute lung injury level among four groups.

Statistical analysis. Statistical differences of the values (virus titers, symptoms, pathological features, cytokines) among four groups were analyzed by an ANOVA multi-comparison test. Statistical analysis was performed with R software version 3.6.2. Student's t-test was used for comparison in the neuraminidase inhibition tests. P values of lower than 0.05 were considered as a statistically significant difference.

Acknowledgement

364 This research is partly supported by Grants-in-Aid for Scientific Research (B) JSPS KAKENHI
365 Grant Number 15H04720, by a grant from the Ministry of Education, Culture, Sports, Science
366 and Technology, Japan for a Joint Research Program of the Research Center for Zoonosis
367 Control, Hokkaido University, and by the Japan Initiative for Global Research Network on
368 Infectious Diseases (J-GRID) of the Japan Agency for Medical Research and Development
369 (AMED) under Grant Number JP 19fm0108008. The funders had no role in study design, data
370 collection and interpretation, or the decision to submit the work for publication. We thank Naoko
371 Kitagawa, Hideaki Ishida, Takako Sasamura and Chikako Kinoshita for their assistance in the
372 experiment and Hideaki Tsuchiya, Shinichiro Nakamura, Takahiro Nakagawa and Ikuo
373 Kawamoto for animal care.
374

375 **References**

376 1. OIE. 2018. OIE Situation Report for Avian Influenza.1-12.
377 2. Li C, Chen H. 2014. Enhancement of influenza virus transmission by gene reassortment.
378 Curr Top Microbiol Immunol 385:185-204.
379 3. Ottmann M, Duchamp MB, Casalegno JS, Frobert E, Moules V, Ferraris O, Valette M,
380 Escuret V, Lina B. 2010. Novel influenza A(H1N1) 2009 in vitro reassortant viruses with
381 oseltamivir resistance. Antivir Ther 15:721-726.
382 4. Neumann G, Noda T, Kawaoka Y. 2009. Emergence and pandemic potential of swine-
383 origin H1N1 influenza virus. Nature 459:931-939.
384 5. OIE. 2017. OIE Situation Report for Avian Influenza 1-14.
385 6. Jiang H, Wu P, Uyeki TM, He J, Deng Z, Xu W, Lv Q, Zhang J, Wu Y, Tsang TK, Kang
386 M, Zheng J, Wang L, Yang B, Qin Y, Feng L, Fang VJ, Gao GF, Leung GM, Yu H,

Cowling BJ. 2017. Preliminary Epidemiologic Assessment of Human Infections With Highly Pathogenic Avian Influenza A(H5N6) Virus, China. Clin Infect Dis 65:383-388.

7. Bi Y, Tan S, Yang Y, Wong G, Zhao M, Zhang Q, Wang Q, Zhao X, Li L, Yuan J, Li H, Li H, Xu W, Shi W, Quan C, Zou R, Li J, Zheng H, Yang L, Liu WJ, Liu D, Wang H, Qin Y, Liu L, Jiang C, Liu W, Lu L, Gao GF, Liu Y. 2019. Clinical and immunological characteristics of human infections with H5N6 avian influenza virus. Clin Infect Dis 68:1100-1109. doi:10.1093/cid/ciy681.

8. Sun H, Pu J, Wei Y, Sun Y, Hu J, Liu L, Xu G, Gao W, Li C, Zhang X, Huang Y, Chang KC, Liu X, Liu J. 2016. Highly Pathogenic Avian Influenza H5N6 Viruses Exhibit Enhanced Affinity for Human Type Sialic Acid Receptor and In-Contact Transmission in Model Ferrets. J Virol 90:6235-6243.

9. Hui KP, Chan LL, Kuok DI, Mok CK, Yang ZF, Li RF, Luk GS, Lee EF, Lai JC, Yen HL, Zhu H, Guan Y, Nicholls JM, Peiris JS, Chan MC. 2017. Tropism and innate host responses of influenza A/H5N6 virus: an analysis of ex vivo and in vitro cultures of the human respiratory tract. Eur Respir J 49:pii: 1601710. doi: 10.1183/13993003.01710-2016.

10. Zhao Z, Guo Z, Zhang C, Liu L, Chen L, Zhang C, Wang Z, Fu Y, Li J, Shao H, Luo Q, Qian J, Liu L. 2017. Avian Influenza H5N6 Viruses Exhibit Differing Pathogenicities and Transmissibilities in Mammals. Sci Rep 7:16280.

11. Herfst S, Mok CKP, van den Brand JMA, van der Vliet S, Rosu ME, Spronken MI, Yang Z, de Meulder D, Lexmond P, Bestebroer TM, Peiris JSM, Fouchier RAM, Richard M. 2018. Human Clade 2.3.4.4 A/H5N6 Influenza Virus Lacks Mammalian Adaptation

409 Markers and Does Not Transmit via the Airborne Route between Ferrets. mSphere 3: pii:
410 e00405-17. doi: 10.1128/mSphere.00405-17.
411 12. Hussain M, Galvin HD, Haw TY, Nutsford AN, Husain M. 2017. Drug resistance in
412 influenza A virus: the epidemiology and management. Infect Drug Resist 10:121-134.
413 13. Gaymard A, Charles-Dufant A, Sabatier M, Cortay JC, Frobert E, Picard C, Casalegno JS,
414 Rosa-Calatrava M, Ferraris O, Valette M, Ottmann M, Lina B, Escuret V. 2016. Impact
415 on antiviral resistance of E119V, I222L and R292K substitutions in influenza A viruses
416 bearing a group 2 neuraminidase (N2, N3, N6, N7 and N9). J Antimicrob Chemother
417 71:3036-3045.
418 14. Fiore AE, Fry A, Shay D, Gubareva L, Bresee JS, Uyeki TM, Centers for Disease C,
419 Prevention. 2011. Antiviral agents for the treatment and chemoprophylaxis of influenza
420 recommendations of the Advisory Committee on Immunization Practices (ACIP).
421 MMWR Recomm Rep 60:1-24.
422 15. Dong G, Peng C, Luo J, Wang C, Han L, Wu B, Ji G, He H. 2015. Adamantane-resistant
423 influenza a viruses in the world (1902-2013): frequency and distribution of M2 gene
424 mutations. PLoS One 10:e0119115.
425 16. Itoh Y, Shichinohe S, Nakayama M, Igarashi M, Ishii A, Ishigaki H, Ishida H, Kitagawa
426 N, Sasamura T, Shiohara M, Doi M, Tsuchiya H, Nakamura S, Okamatsu M, Sakoda Y,
427 Kida H, Ogasawara K. 2015. Emergence of H7N9 Influenza A Virus Resistant to
428 Neuraminidase Inhibitors in Nonhuman Primates. Antimicrob Agents Chemother
429 59:4962-4973.
430 17. Arikata M, Itoh Y, Okamatsu M, Maeda T, Shiina T, Tanaka K, Suzuki S, Nakayama M,
431 Sakoda Y, Ishigaki H, Takada A, Ishida H, Soda K, Pham VL, Tsuchiya H, Nakamura S,

Torii R, Shimizu T, Inoko H, Ohkubo I, Kida H, Ogasawara K. 2012. Memory immune responses against pandemic (H1N1) 2009 influenza virus induced by a whole particle vaccine in cynomolgus monkeys carrying Mafa-A1*052:02. PLoS One 7:e37220.

18. Pham VL, Nakayama M, Itoh Y, Ishigaki H, Kitano M, Arikata M, Ishida H, Kitagawa N, Shichinohe S, Okamatsu M, Sakoda Y, Tsuchiya H, Nakamura S, Kida H, Ogasawara K. 2013. Pathogenicity of pandemic H1N1 influenza A virus in immunocompromised cynomolgus macaques. PLoS One 8:e75910.

19. Hiono T, Okamatsu M, Matsuno K, Haga A, Iwata R, Nguyen LT, Suzuki M, Kikutani Y, Kida H, Onuma M, Sakoda Y. 2017. Characterization of H5N6 highly pathogenic avian influenza viruses isolated from wild and captive birds in the winter season of 2016-2017 in Northern Japan. Microbiol Immunol 61:387-397.

20. Okamatsu M, Ozawa M, Soda K, Takakuwa H, Haga A, Hiono T, Matsuu A, Uchida Y, Iwata R, Matsuno K, Kuwahara M, Yabuta T, Usui T, Ito H, Onuma M, Sakoda Y, Saito T, Otsuki K, Ito T, Kida H. 2017. Characterization of Highly Pathogenic Avian Influenza Virus A(H5N6), Japan, November 2016. Emerg Infect Dis 23:691-695.

21. Choi WS, Jeong JH, Kwon JJ, Ahn SJ, Lloren KKS, Kwon HI, Chae HB, Hwang J, Kim MH, Kim CJ, Webby RJ, Govorkova EA, Choi YK, Baek YH, Song MS. 2018. Screening for Neuraminidase Inhibitor Resistance Markers among Avian Influenza Viruses of the N4, N5, N6, and N8 Neuraminidase Subtypes. J Virol 92:pii: e01580-17. doi: 10.1128/JVI.01580-17.

22. De Jong MD, Ison MG, Monto AS, Metev H, Clark C, O'Neil B, Elder J, McCullough A, Collis P, Sheridan WP. 2014. Evaluation of intravenous peramivir for treatment of influenza in hospitalized patients. Clin Infect Dis 59:e172-85.

455 23. Yang. Z-F, Mok. CKP, Peiris. JSM, Zhong. N-S. 2015. Human Infection with a Novel
456 Avian Influenza A(H5N6) Virus. N Engl J Med 373:487-489.
457 24. Shieh WJ, Blau DM, Denison AM, Deleon-Carnes M, Adem P, Bhatnagar J, Sumner J,
458 Liu L, Patel M, Batten B, Greer P, Jones T, Smith C, Bartlett J, Montague J, White E,
459 Rollin D, Gao R, Seales C, Jost H, Metcalfe M, Goldsmith CS, Humphrey C, Schmitz A,
460 Drew C, Paddock C, Uyeki TM, Zaki SR. 2010. 2009 pandemic influenza A (H1N1):
461 pathology and pathogenesis of 100 fatal cases in the United States. Am J Pathol 177:166-
462 175.
463 25. Liem NT, Nakajima N, Phat le P, Sato Y, Thach HN, Hung PV, San LT, Katano H,
464 Kumasaka T, Oka T, Kawachi S, Matsushita T, Sata T, Kudo K, Suzuki K. 2008. H5N1-
465 infected cells in lung with diffuse alveolar damage in exudative phase from a fatal case in
466 Vietnam. Jpn J Infect Dis 61:157-160.
467 26. Feng Y, Hu L, Lu S, Chen Q, Zheng Y, Zeng D, Zhang J, Zhang A, Chen L, Hu Y,
468 Zhang Z. 2015. Molecular pathology analyses of two fatal human infections of avian
469 influenza A(H7N9) virus. J Clin Pathol 68:57-63.
470 27. Gao R, Pan M, Li X, Zou X, Zhao X, Li T, Yang H, Zou S, Bo H, Xu J, Li S, Zhang M,
471 Li Z, Wang D, Zaki SR, Shu Y. 2016. Post-mortem findings in a patient with avian
472 influenza A (H5N6) virus infection. Clin Microbiol Infect 22:574 e1-5.
473 28. Betakova T, Kostrabova A, Lachova V, Turianova L. 2017. Cytokines Induced During
474 Influenza Virus Infection. Curr Pharm Des 23:2616-2622.
475 29. Van Reeth K. 2000. Cytokines in the pathogenesis of influenza. Vet Microbiol 74:109-
476 116.

30. Kitano M, Itoh Y, Ishigaki H, Nakayama M, Ishida H, Pham VL, Arikata M, Shichinohe S, Tsuchiya H, Kitagawa N, Kobayashi M, Yoshida R, Sato A, Le QM, Kawaoka Y, Ogasawara K. 2014. Efficacy of repeated intravenous administration of peramivir against highly pathogenic avian influenza A (H5N1) virus in cynomolgus macaques. Antimicrob Agents Chemother 58:4795-4803.

31. De Jong MD, Simmons CP, Thanh TT, Hien VM, Smith GJ, Chau TN, Hoang DM, Chau NV, Khanh TH, Dong VC, Qui PT, Cam BV, Ha do Q, Guan Y, Peiris JS, Chinh NT, Hien TT, Farrar J. 2006. Fatal outcome of human influenza A (H5N1) is associated with high viral load and hypercytokinemia. Nat Med 12:1203-1207.

32. Szretter KJ, Gangappa S, Belser JA, Zeng H, Chen H, Matsuoka Y, Sambhara S, Swayne DE, Tumpey TM, Katz JM. 2009. Early control of H5N1 influenza virus replication by the type I interferon response in mice. J Virol 83:5825-5834.

33. Liu Q, Ma J, Strayer DR, Mitchell WM, Carter WA, Ma W, Richt JA. 2014. Emergence of a novel drug resistant H7N9 influenza virus: evidence based clinical potential of a natural IFN-alpha for infection control and treatment. Expert Rev Anti Infect Ther 12:165-169.

34. Sato M, Hashimoto K, Kawasaki Y, Hosoya M. 2018. Immune response after a single intravenous peramivir administration in children with influenza. Antivir Ther 23:435-441.

35. Ilyushina NA, Govorkova EA, Russell CJ, Hoffmann E, Webster RG. 2007. Contribution of H7 haemagglutinin to amantadine resistance and infectivity of influenza virus. J Gen Virol 88:1266-1274.

498 36. Togo Y, Hornick RB, Felitti VJ, Kaufman ML, Dawkins AT, Jr., Kilpe VE, Claghorn JL.
499 1970. Evaluation of therapeutic efficacy of amantadine in patients with naturally
500 occurring A2 influenza. JAMA 211:1149-1156.
501 37. Kandeil A, Kayed A, Moatasim Y, Webby RJ, McKenzie PP, Kayali G, Ali MA. 2017.
502 Genetic characterization of highly pathogenic avian influenza A H5N8 viruses isolated
503 from wild birds in Egypt. J Gen Virol 98:1573-1586.
504 38. Levite M. 2016. Dopamine and T cells: dopamine receptors and potent effects on T cells,
505 dopamine production in T cells, and abnormalities in the dopaminergic system in T cells
506 in autoimmune, neurological and psychiatric diseases. Acta Physiol (Oxf) 216:42-89.
507 39. Kocks JR, Davalos-Misslitz AC, Hintzen G, Ohl L, Forster R. 2007. Regulatory T cells
508 interfere with the development of bronchus-associated lymphoid tissue. J Exp Med
509 204:723-734.
510 40. Kitano M, Itoh Y, Kodama M, Ishigaki H, Nakayama M, Nagata T, Ishida H, Tsuchiya H,
511 Torii R, Baba K, Yoshida R, Sato A, Ogasawara K. 2010. Establishment of a cynomolgus
512 macaque model of influenza B virus infection. Virology 407:178-184.
513 41. Chen F, Liu Z, Wu W, Rozo C, Bowdridge S, Millman A, Van Rooijen N, Urban JF, Jr.,
514 Wynn TA, Gause WC. 2012. An essential role for TH2-type responses in limiting acute
515 tissue damage during experimental helminth infection. Nat Med 18:260-266.
516

517 **Table 1. Virus titers in swab samples of cynomolgus macaques infected with H5N6 and**

518 **treated with antiviral drugs.**

Sample [a]	Treatment	Animal	Virus titers ($Log_{10}TCID_{50}$/mL)						
			Days after virus inoculation						
			1	2	3	4	5	6	7
Nasal swab	Saline	S1[b]	3.50	2.67	[c] <	[e] ≤ 0.83	2.50	2.67	[h] ≤ 1.33
		S2	3.83	3.23	1.83	2.00	3.44	4.83	3.00
		S3	[d] ≤ 0.67	1.50	2.33	3.50	3.50	3.67	3.23
	Oseltamivir	O1	3.50	1.50	≤ 0.67	<	<	<	<
		O2	3.83	≤ 0.67	2.00	[j] ≤ 1.5	[g] ≤ 1.23	<	<
		O3	<	≤ 1.33	<	<	<	<	<
	Peramivir	P1	≤ 1.33	<	<	<	<	<	<
		P2	3.50	[f] ≤ 1.00	≤ 1.00	<	<	≤ 0.67	<
		P3	4.00	< 0.67	< 1.00	<	<	<	<
	Amantadine	A1	3.50	1.67	2.23	2.50	2.23	[l] ≤ 1.77	<
		A2	≤ 1.33	<	≤ 1.50	≤ 1.77	2.50	2.33	≤ 1.00
		A3	≤ 1.33	<	<	<	<	<	<
Trachea swab	Saline	S1	4.67	3.33	<	1.67	2.00	≤ 0.67	<
		S2	3.67	≤ 1.00	<	<	≤ 0.67	≤ 0.67	<
		S3	<	2.50	2.50	≤ 0.75	1.83	≤ 0.67	≤ 0.67
	Oseltamivir	O1	2.67	2.83	[m] ≤ 1.83	≤ 0.83	<	<	<
		O2	3.50	2.00	2.00	2.50	<	<	<
		O3	4.33	3.77	2.33	<	<	<	<
	Peramivir	P1	2.5	2.67	≤ 1.5	[i] ≤ 1.44	< 1	<	<
		P2	4.00	≤ 1.00	≤ 1.44	<	<	<	<
		P3	4.50	2.77	20	1.83	<	<	<
	Amantadine	A1	5.67	2.50	[n] ≤ 2.17	3.33	2.67	≤ 1.23	<
		A2	4.50	[k] ≤ 1.67	≤1.00	≤ 1.50	2.63	≤ 1.50	<
		A3	4.67	3.50	<	2.33	3.50	<	2.23
Bronchial swab	Saline	S1	3.67	4.00	1.67	2.83	1.50	2.67	<
		S2	5.00	3.00	≤ 1.00	≤ 1.00	1.67	≤ 1.50	<
		S3	2.00	<	2.50	2.67	2.23	1.50	<
	Oseltamivir	O1	1.83	2.50	2.00	<	≤ 0.67	<	<
		O2	4.00	≤ 1.00	<	2.23	≤ 0.83	<	<
		O3	3.33	2.50	≤ 1.23	<	≤ 0.67	<	<

	Peramivir	P1	3.00	2.50	2.00	≤ 1.50	≤ 1.00	<	<
		P2	4.33	3.50	≤ 0.67	<	<	<	<
		P3	4.67	3.00	<	1.38	<	<	<
	Amantadine	A1	3.67	3.00	≤ 1.00	≤ 1.00	2.23	<	<
		A2	4.50	≤ 1.23	≤ 1.77	< 1.50	3.50	[o] ≤ 2.25	<
		A3	4.00	2.33	≤ 1.33	3.23	3.00	2.25	≤ 1.00

519

520 [a] : Sampling organs.

521 [b] : Macaque identification.

522 [c] <: No CPE-positive well in quadruplicate culture. A detection limit was 0.67 $\log_{10}TCID_{50}$/mL.

523 [d] ≤ 0.67: One CPE-positive well in quadruplicate culture with the undiluted samples was
524 observed.

525 [e] ≤ 0.83: Two CPE-positive wells were observed in quadruplicate culture: one with undiluted
526 samples and one with 10-fold diluted sample.

527 [f] ≤ 1: Two CPE-positive wells in quadruplicate culture with undiluted sample were observed.

528 [g] ≤1.23: Three CPE-positive wells were observed in quadruplicate culture: two with undiluted
529 sample and one with 10-fold diluted sample.

530 [h] ≤1.33: Three CPE-positive wells in quadruplicate culture with undiluted sample were observed.

531 [i] ≤ 1.44: Four CPE-positive wells were observed in quadruplicate culture: two with undiluted
532 sample; one with 10-fold diluted sample and one with 100-fold diluted sample.

533 [j] ≤ 1.5: Four CPE-positive wells were observed in quadruplicate culture: two with undiluted
534 sample and two with 10-fold diluted sample.

535 [k] ≤ 1.67: Five CPE-positive wells were observed in quadruplicate culture: three with undiluted
536 sample; one with 10-fold diluted sample and one with 1000-fold diluted sample.

537 [l] ≤ 1.77: Five CPE-positive wells were observed in quadruplicate culture: three with undiluted
538 sample and two with 10-fold diluted sample.

539 [m] ≤ 1.83: Six CPE-positive wells were observed in quadruplicate culture: three with undiluted
540 sample; one with 10-fold diluted sample and two with 100-fold diluted sample.

541 [n] ≤ 2.17: Six CPE-positive wells were observed in quadruplicate culture: three with undiluted
542 sample; three with 10-fold diluted sample.

543 [o] ≤ 2.25: Seven CPE-positive wells were observed in quadruplicate culture: three with undiluted
544 sample; two with 10-fold diluted sample and two with 100-fold diluted sample.

Figure legends

Fig 1. Symptoms of cynomolgus macaques challenged with A/black swan/Akita/1/2016 (H5N6).

Cynomolgus macaques (n = 3) were inoculated with the virus on day 0. (a) Averages and standard deviations of body temperature and (b) heart rate were determined by using a telemetry probe system during the night (from 8:00 p.m. to 8:00 a.m.) and data were adjusted to day -1. (c, d) Averages and standard deviations of food consumption and body weight are shown. (c) Food consumption was estimated by the following formation: food consumption = [(number of pellets given in the morning - number of pellets left at night)/number of pellets given in the morning] × 100 (%). (d) Body weight was monitored every day. Statistical differences among groups are calculated with an ANOVA multi-comparison test.

Fig 2. Viral pneumonia in cynomolgus macaques challenged with A/black swan/Akita/1/2016 (H5N6).

H&E staining of lung tissues collected 7 days after virus infection. Representative photos of cynomolgus macaques treated with saline (a), oseltamivir (b), peramivir (c) and amantadine (d). Black arrow heads point neutrophils. Bars, 50 μm.

Fig 3. Peripheral blood cell populations and cytokine/chemokine responses in cynomolgus macaques challenged with A/black swan/Akita/1/2016 (H5N6).

(a-d) Concentrations in peripheral blood cells collected on the indicated days: (a) total leukocytes, (b) granulocytes, (c) monocytes, and (d) lymphocytes. (e-h) Levels of cytokines/chemokines in plasma after virus infection. The average values and standard deviations were shown.

Fig 4. Efficacy of antiviral drugs against A/black swan/Akita/1/2016 (H5N6) virus *in vitro*.

MDCK cells were infected with the virus at a multiplicity of infection (MOI) of 0.01 and cultured with antiviral drugs of various concentrations: (a) oseltamivir, (b, d) peramivir, and (c) amantadine. Sensitivity of the inoculum virus (a-c) and the virus recovered from a tonsil of macaque P2 on day 7 (d) was examined. The supernatant of each well was collected at 24 h and 48 h after virus infection. Then virus titers in the supernatants were determined by the Reed Muench method. Averages and standard deviations of three independent experiments were shown in a-c. Averages and standard deviations of triplicate culture were shown in d. EC_{50} values were calculated by "Quest Graph™ EC50 Calculator." *AAT Bioquest, Inc*, 03 Feb. 2020, https://www.aatbio.com/tools/ec50-calculator. The asterisks show significant differences in virus titers with treatment at each antiviral drug concentration and without treatment (0 μg/mL) (Student's t-test, *: $P < 0.05$, **:$P<0.01$).

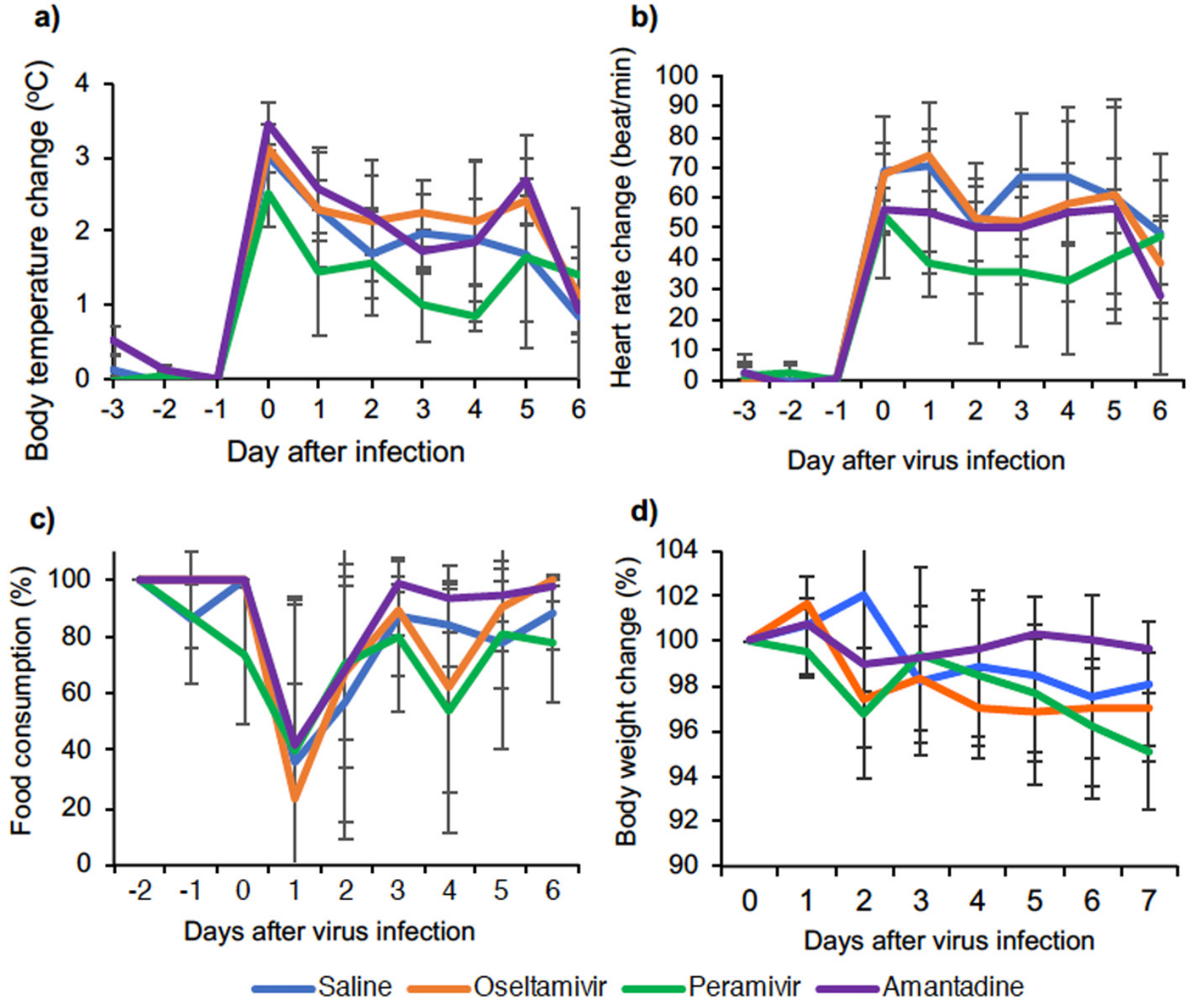
a)
Body temperature change (°C)
Day after infection
b)
Heart rate change (beat/min)
Day after virus infection
c)
Food consumption (%)
Days after virus infection
d)
Body weight change (%)
Days after virus infection
Saline
Oseltamivir
Peramivir
Amantadine

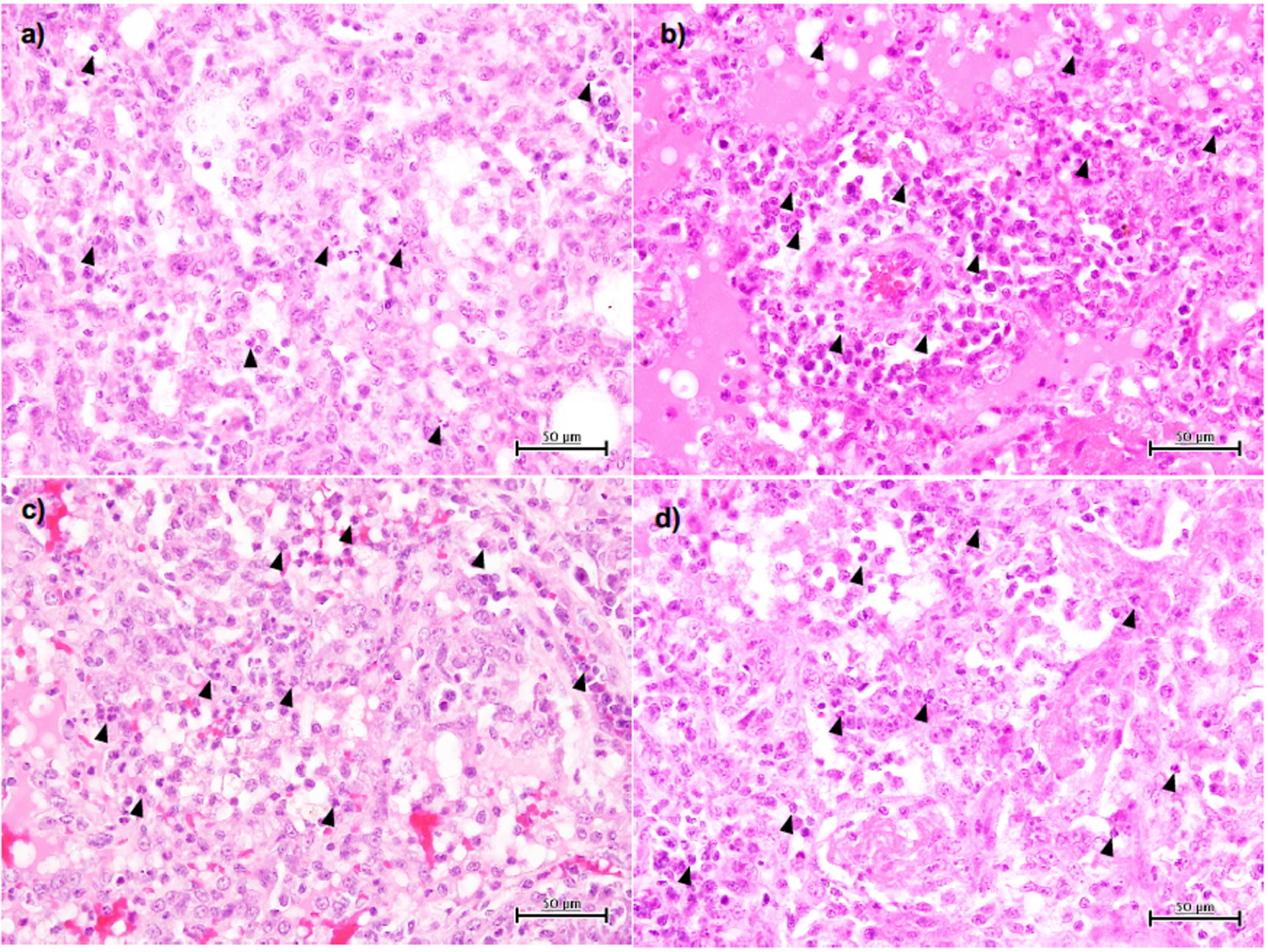
a)
50 µm
b)
50 µm
c)
50 µm
d)
50 µm

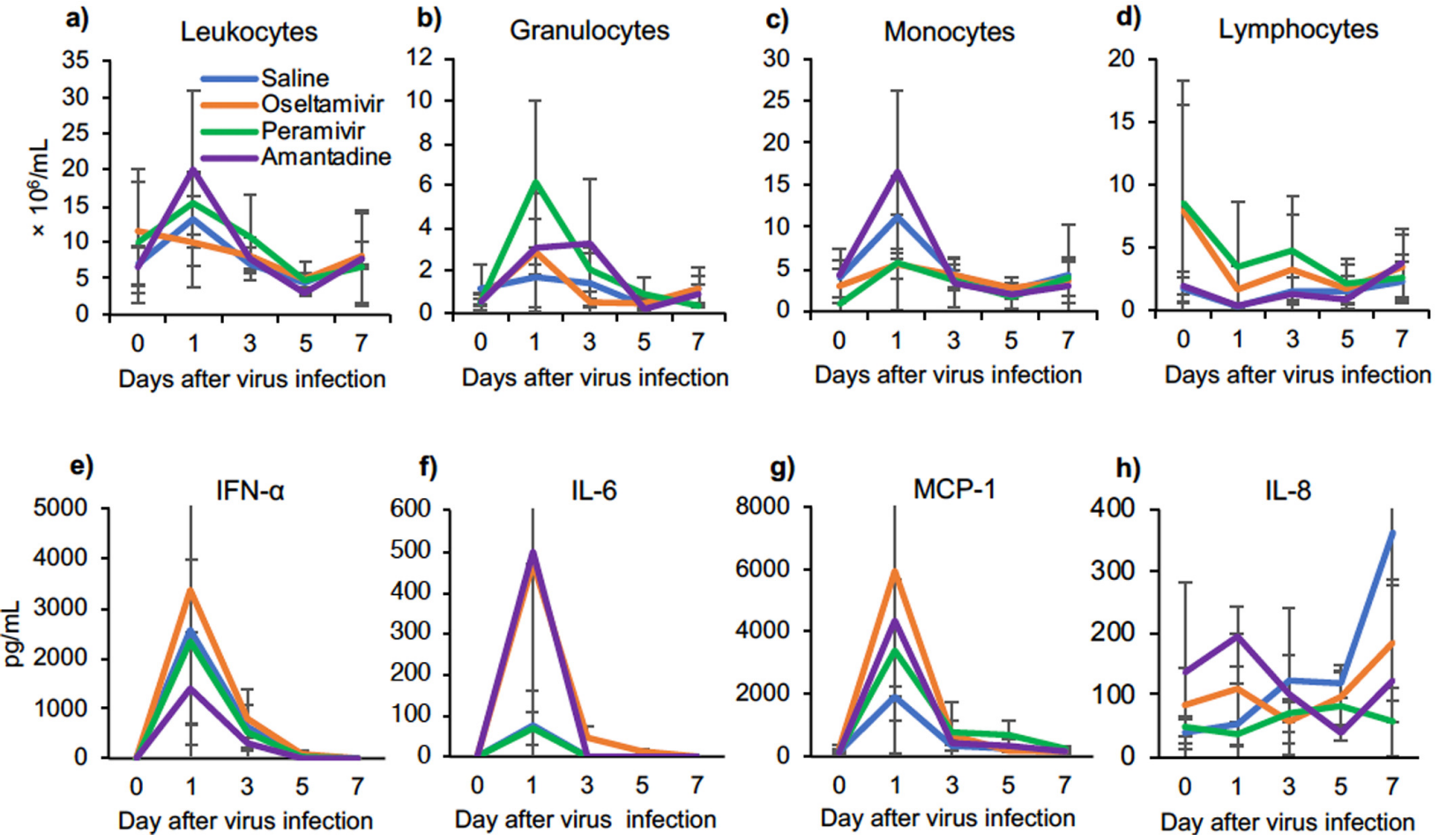
a)
Leukocytes
× 10⁶/mL
Saline
Oseltamivir
Peramivir
Amantadine
Days after virus infection
b)
Granulocytes
Days after virus infection
c)
Monocytes
Days after virus infection
d)
Lymphocytes
Days after virus infection
e)
IFN-α
pg/mL
Day after virus infection
f)
IL-6
Day after virus infection
g)
MCP-1
Day after virus infection
h)
IL-8
Day after virus infection

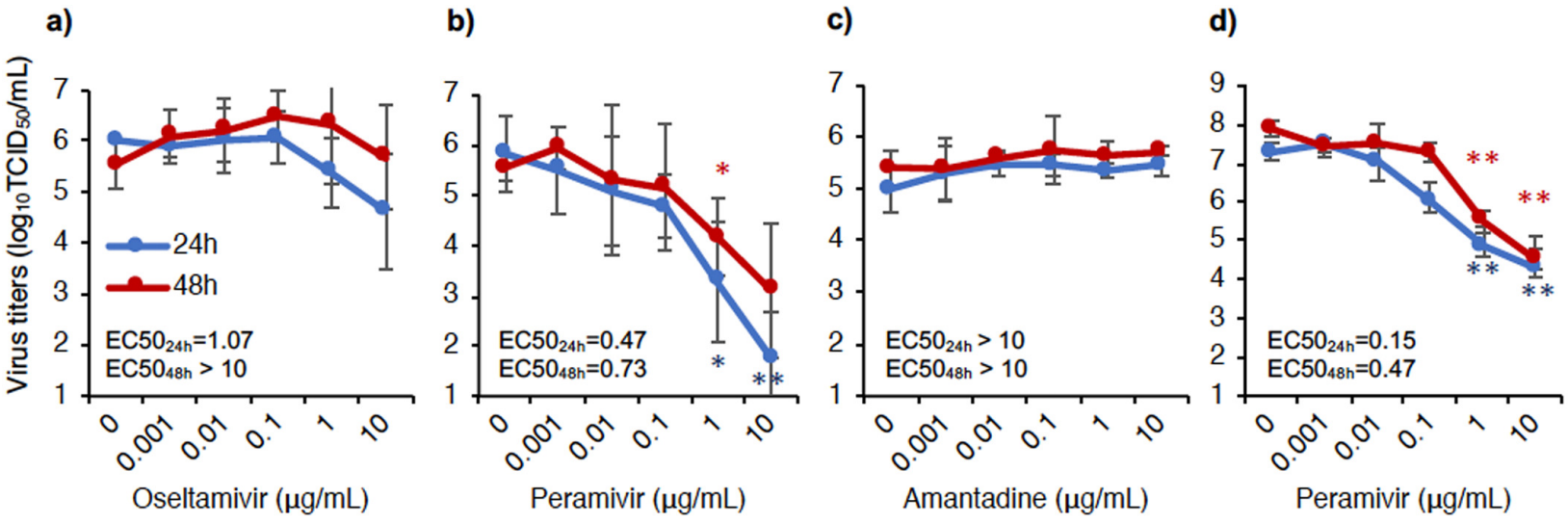
a)
b)
c)
d)
Virus titers ($log_{10}TCID_{50}$/mL)
24h
48h
$EC50_{24h}$=1.07
$EC50_{48h}$ > 10
$EC50_{24h}$=0.47
$EC50_{48h}$=0.73
$EC50_{24h}$ > 10
$EC50_{48h}$ > 10
$EC50_{24h}$=0.15
$EC50_{48h}$=0.47
0
0.001
0.01
0.1
1
10
Oseltamivir (μg/mL)
Peramivir (μg/mL)
Amantadine (μg/mL)
Peramivir (μg/mL)